J. Phys. B: At. Mol. Opt. Phys. **29** (1996) 4675–4687. Printed in the UK

Single electron transfer and target excitation in $He^{2+} + Na$ (3s) collisions at 2–50 keV amu^{-1} in the coupled-Sturmian-pseudostate approach

Ashok Jain and Thomas G Winter

Physics Department, Pennsylvania State University, Wilkes-Barre Campus, Lehman, Pennsylvania 18627, USA

Received 30 January 1996, in final form 29 May 1996

Abstract. A two-centre coupled-Sturmian-pseudostate approach is employed to calculate single electron transfer, target excitation and total ionization cross sections for the $He^{2+} + Na$ (3s) collision system at 2–50 keV amu^{-1} impact energies. The Sturmian basis set, together with an analytic Hartree–Fock potential for the Na core, are chosen carefully so that all three channels (transfer, excitation and ionization) are included in the coupled scheme. The present state-selective and total charge transfer cross sections compare fairly well with experimental data, as well as with previous theoretical results, particularly below 10 keV amu^{-1}. The target excitation cross sections for the sodium 3p and 4d states are in very good agreement with the available measurements, while significant discrepancy exists between theory and experiment for the excitation of the Na (4p) state.

1. Introduction

Recently (Jain and Winter 1995), we employed the coupled-Sturmian-pseudostate method (Winter 1982, 1987, 1993a, b) to determine electron transfer, target excitation and ionization cross sections for the quasi-one-electron $H^+ + Na$ (3s and 3p) collision at 1–100 keV impact energies. A total of 70 states were included on both the atomic centres in order to account for electron transfer (up to the $n = 3$ state of H), target excitation (3p, 3d, 4s, 4p, and 4d states of Na), and ionization channels. In this application of the coupled Sturmian method to the $H^+ + Na$ system, a large number of coupled channels were needed in order to account for important components in the inelastic processes of electron transfer, target excitation and ionization. These results for the $H^+ + Na$ (3s and 3p) collision system were found to be in very good agreement with experimental and well as with other calculations for almost all the inelastic channels, as mentioned above.

The coupled-Sturmian-pseudostate basis has the advantages of being systematic, square integrable, and, in principle, complete, if the basis is sufficiently large. In order to see further the applicability of the coupled Sturmian approach, we have now studied the collision system $He^{2+} + Na$ (3s) for the three processes (electron transfer, target excitation and ionization) in the range of 2–50 keV amu^{-1}, where experimental and theoretical data are available for comparison. In the $H^+ + Na$ (3s) case (Jain and Winter 1995), capture to 4f sublevels of H is not an important channel and therefore was neglected in the coupled treatment; however, for the present $He^{2+} + Na$ (3s) case, capture to the 4f sublevels of the He^+ ion is quite significant below about 15 keV amu^{-1} (showing peaking behaviour around 5 keV amu^{-1})

0953-4075/96/204675+13$19.50

(see Schippers *et al* 1995). One needs to increase the size of the Sturmian basis set. Thus the present application of the coupled Sturmian method is even more challenging.

Another reason to carry out the present calculations is that for the collision of multiply charged He^{2+} ions with Na(3s), little work has been done, either theoretically or experimentally. This collision system has many practical applications such as in short wavelength lasers and fusion plasmas. So far, to the best of our knowledge, there are only two sets of theoretical calculations for the $He^{2+} + Na$ (3s) system: one, by Shingal *et al* (1987), who have reported single electron transfer and target excitation cross sections in the energy range of 2.5–66 keV amu^{-1} using an augmented atomic-orbital (AO) approach; the other, by Kumar *et al* (1990), who have calculated total charge transfer cross sections in the 0.1–10 keV amu^{-1} energy range using the semiclassical molecular expansion method. To the best of our knowledge, the only calculation available for target excitation in $He^{2+} + Na$ (3s) collisions is the one by Shingal *et al* (1987).

Experimentally, total charge transfer cross sections have been measured by DuBois and Toburen (1985) and DuBois (1986) from low to intermediate energies (1–50 keV amu^{-1}). At much lower energies (0.125–1.5 keV amu^{-1}), Schweinzer and Winter (1990) have measured total electron capture from alkali atoms (Li, Na and K) by He^{2+} ions. Schweinzer and Winter have also calculated these cross sections by employing semiclassical atomic expansion close coupling and purely classical methods. Total cross sections for excitation to the Na(3p) state have been measured by Dehong *et al* (1989) in the range of 15–70 keV amu^{-1}, while Schlatmann *et al* (1992) have reported their measured values for single electron transfer and target excitation channels in an energy range of 2–9 keV amu^{-1}. More recently, Schippers *et al* (1995) have measured profiles and the linear polarization of the He^{+} $(4 \rightarrow 3)$ emission in the $He^{2+} + Na$ (3s) collision at 2–13.3 keV amu^{-1}; they compared these results on the polarization and emission cross section parameters with their calculations using the classical trajectory Monte Carlo (CTMC) method. Several experiments have also been carried out on He^{2+} collisions with aligned and oriented Na(3p) atoms (Aumayr *et al* 1991, Gieler *et al* 1993). The final goal of this study is to obtain information on the full density matrix for the $He^{2+} + Na$ (3s and 3p) system in the present energy regime.

The outline of the paper is as follows. In section 2, the theoretical method and numerical procedure are summarized, while in section 3, all the cross sections will be presented and compared with experimental data and previous calculations. Concluding remarks will be made in section 4. Atomic units are used unless otherwise specified.

2. Theoretical model

The details of the theoretical model are the same as those given in our earlier paper on charge transfer and target excitation in $H^{+} + Na$ (3s and 3p) collisions (Jain and Winter 1995) and will not be repeated here. Here we provide only a brief description of the basis set (which is slightly different from the corresponding $H^{+} + Na$ (3s and 3p) one).

The Sturmian basis for the $He^{2+} + Na$ (3s) case is quite similar to that for $H^{+} + Na$ (3s and 3p) except that in the present case we have included 4f functions on the He^{2+} centre. In order to get the correct energy spectrum on each centre we have chosen 82 terms (14sB/9pB/5dB/14sA/9pA/5dA/4fA) for the Sturmian basis. Here A and B represent respectively the He^{2+} and Na centres. However, the number of coupled equations with this 82-term Sturmian basis on both centres is only 74 (excluding 1sB, 2sB, 2pB, 13sB, 14sB, 13sA, 14sA) after diagonalizing the Hamiltonians. The ionization channels are described by the discrete functions 5s–12s, 6p–9p, and 5d on each centre, lying in the continuum with

positive energy eigenvalues up to 14.32 au and 2.57 au on the projectile and target centres respectively.

For full details on the convergence and various integration schemes, we refer to our earlier paper (Jain and Winter 1995). In the present problem of solving the 74 coupled equations, we kept largely the same convergence criterion for various integrations as in that paper.

We did carry out additional tests on the sensitivity of probabilities with respect to various sizes of basis and number of coupled equations; we checked the convergence of probabilities at the energy 10 keV amu^{-1} and the impact parameter $b = 0.25$ au with respect to 70-state and 74-state calculations. We compared various probabilities using 65-state, 70-state, and 74-state coupled channels; the dominant channels on both the centres converged to within 10%. Due to computer time limitations, it was not possible to carry out additional convergence tests with respect to basis size.

Table 1. Present 70-state (without capture to 4f sublevel) and 74-state (with capture to 4f sublevel) calculations for various cross sections (10^{-16} cm^2) for He^{2+} + Na (3s) collisions at 10 keV amu^{-1}.

Cross Section	70-State	74-State
σ_{cap}^{tot}	64.94	76.74
σ_{exc}^{tot}	80.61	68.58
$\sigma_{cap}^{n=2}$	0.74	0.73
$\sigma_{cap}^{n=3}$	43.50	43.02
$\sigma_{cap}^{n=4}$	16.56	28.77
σ_{cap}^{4f}	—	5.37
σ_{exc}^{3p}	56.77	49.30
σ_{exc}^{3d}	9.24	8.23
σ_{exc}^{4p}	7.85	6.11
σ_{exc}^{4d}	13.05	12.39

In table 1, we have shown various charge transfer and target excitation cross sections with (74-state) and without (70-state) the 4f orbitals on the projectile centre. The inclusion of 4f states in the capture channel reduces (by about 15%) the total excitation cross section by almost the same amount as the increase (about 20%) in the total capture cross section. It is interesting to note that the $n = 2$ and $n = 3$ transfer cross sections are unaffected by the inclusion of 4f substates. However, the corresponding reductions in the target excitation channels due to the inclusion of the 4f orbital on the He^+ centre are about 13%, 11%, 22%, and 5% for the sodium 3p, 3d, 4p, and 4d excitations, respectively.

Our final 74-state results are probably converged to within 10% accuracy with few exceptions, including the ionization cross sections, which are probably converged to within 25% accuracy.

3. Results and discussion

3.1. Single electron transfer cross sections for $He^{2+} + Na$ (3s) collisions

We now discuss our final cross sections (transfer, excitation, and ionization) using the potential of equation (1) of Jain and Winter (1995) for the active electron and the Na core. Total cross sections for the single electron transfer (σ_{cap}^{tot}) in He^{2+} + Na (3s) collisions are shown in figure 1 along with the experimental data of DuBois and Toburen (1985)

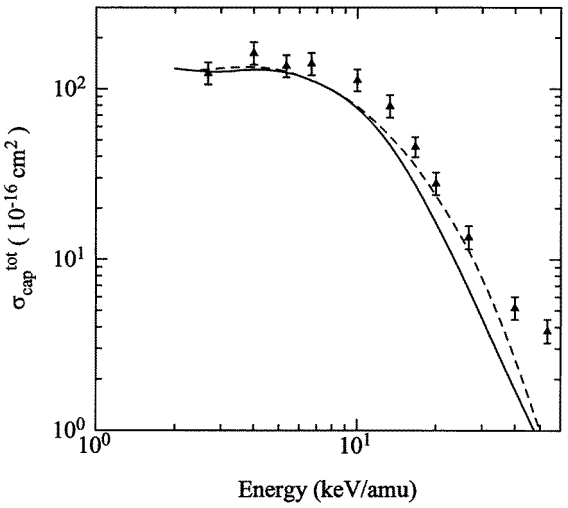

Figure 1. Total single electron transfer cross sections (σ_{cap}^{tot})(10^{-16} cm^2) for the $He^{2+} + Na$ (3s) system in the energy range of 2–50 keV amu^{-1}. Theory: full curve, present Sturmian results; broken curve, Shingal *et al* (1987). Experimental points are taken from DuBois and Toburen (1985).

and the augmented AO calculations of Shingal *et al* (1987). It should be noted that their calculations employ the same Hartree–Fock potential (1) as we use; only the bases are different. All the results, theoretical as well as experimental, shown in figure 1, are in good agreement at the lower energies. In particular, the general behaviour of σ_{cap}^{tot} as a function of impact energy is well reproduced by both theoretical curves. In addition, a broad peaking structure around 4–5 keV amu^{-1} is present in all the data, theoretical and experimental. Above 10 keV amu^{-1}, the σ_{cap}^{tot} values decrease rapidly with an increase in energy. Above this energy, there is significant discrepancy between present theory and the measurements of DuBois and Toburen (1985). Augmented AO results of Shingal *et al* (1987) in the 10–30 keV amu^{-1} region seem to agree with the measurements better than the present results. Above the 30 keV amu^{-1} energy, both theoretical results are much smaller than the experimental data of DuBois and Toburen (1985). The reason for this rather large discrepancy between theory and experiment may be the fact that at such high energies, capture and ionization from inner shells (mostly the L shell) plays a significant role in the collision dynamics.

The state-selective electron transfer cross sections to various $He^+(n\ell)$ states are given in table 2 in the present energy range of 2–50 keV amu^{-1}. Experimental data are available only below 10 keV amu^{-1} for the $He^+(n = 3)$ and $He^+(n = 4)$ states, which we have plotted in figures 2 and 3, respectively. Our theoretical results are in good agreement with the measurements of Schlatmann *et al* (1992). In particular, in figure 2 for the $He^+(n = 3)$ case, the experimental points seem to have a hump around 4 keV amu^{-1}, which is also present in our curve. From figure 2, we see clearly that the present Sturmian results are better in shape than the augmented AO results of Shingal *et al* (1987), when both calculations are compared with the measurements. This is particularly true for the $He^+(n = 4)$ cross sections also (figure 3), where we find that the present Sturmian results compare qualitatively very well with the experimental data. The 6–7 keV amu^{-1} peak present in the augmented AO results of Shingal *et al* (1987) is not found either in the present curve or in the measurements.

Table 2. Present 74-state electron transfer cross sections (10^{-16} cm^2) for He^{2+} + Na (3s) collisions.

Energy (keV amu^{-1})	2s	2p	3s	3p	3d	4s	4p	4d	4f	Total
2.0	0.21	0.67	9.07	29.80	75.69	1.10	5.21	5.64	3.71	131.86
3.0	0.24	0.71	5.02	23.28	71.58	0.79	5.32	10.06	8.17	126.43
4.0	0.23	0.50	4.80	21.67	72.55	0.67	4.89	13.29	10.06	129.77
5.0	0.21	0.51	4.40	19.45	68.51	0.77	6.10	13.86	11.48	126.99
6.0	0.18	0.50	3.96	16.88	62.48	0.91	8.01	13.94	10.42	119.27
7.0	0.185	0.53	3.20	14.57	54.16	0.99	9.84	13.60	9.04	108.59
8.0	0.19	0.52	2.63	12.36	46.59	0.94	10.16	13.77	7.45	97.95
10.0	0.21	0.52	1.66	8.95	32.42	0.95	10.06	12.39	5.37	76.74
12.5	0.21	0.58	0.91	5.65	19.90	0.82	7.74	10.04	3.48	53.22
15.0	0.17	0.57	0.48	3.52	12.35	0.58	5.13	7.78	2.27	35.77
20.0	0.14	0.44	0.15	1.31	4.98	0.28	2.49	3.95	0.98	16.36
25.0	0.13	0.31	0.078	0.58	2.31	0.15	1.05	2.09	0.49	8.23
30.0	0.11	0.22	0.05	0.33	1.16	0.09	0.47	1.18	0.27	4.50
40.0	0.071	0.134	0.033	0.16	0.037	0.04	0.20	0.42	0.10	1.74
50.0	0.051	0.08	0.025	0.075	0.14	0.027	0.11	0.18	0.04	0.85

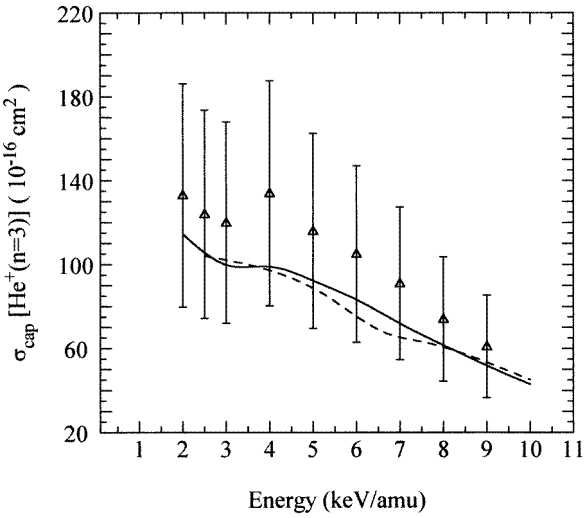

Figure 2. Cross sections as in figure 1, but for the state-selective electron transfer to the $n = 3$ shell of the He^+ ion. The experimental points (triangles) are taken from Schlatmann *et al* (1992).

Both calculations for the $He^+(n = 4)$ channel, presented in figure 3, seem to overestimate the measured values, but ours only slightly.

As mentioned earlier, unlike for the H^+ + Na (3s) case, electron transfer to the He^+ (4f) state is a significant channel which has a peaking behaviour at about 5 keV amu^{-1}. The electron transfer to He^+ (4f) is illustrated in figure 4 along with other results as depicted in figure 3 of Schippers *et al* 1995. Very recently, Schippers *et al* (1995) have used the measurements of Schlatmann *et al* (1992) to extract partial cross sections for He^+ (4f) capture. Near this peak, the He^+ (4f) cross section is about 10% of the total capture cross section. In this low energy region (below 6 keV amu^{-1}), capture to the 4d and 4f subshells

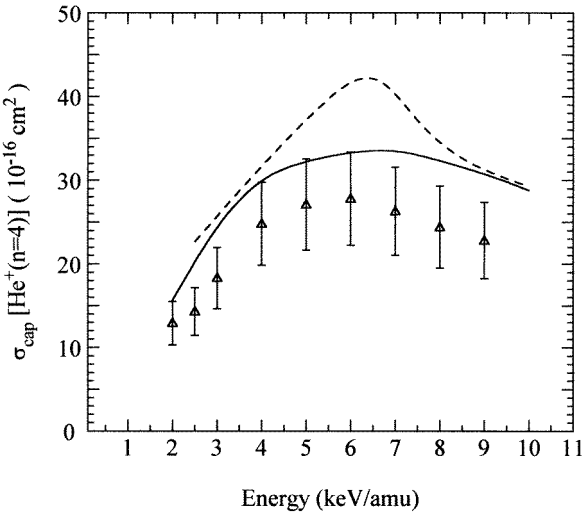

Figure 3. Same figure caption as in figure 1, but for the state-selective electron transfer to the $n = 4$ shell of the He^+ ion.

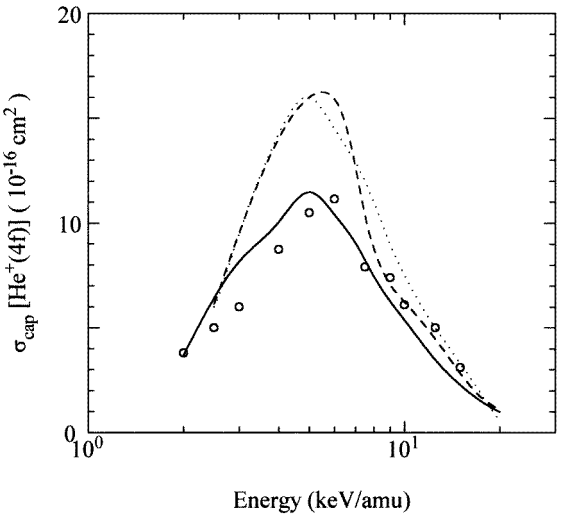

Figure 4. Partial electron transfer cross sections into the 4f shell of He^+. Full curve, present Sturmian results; broken curve, Shingal *et al* (1987); dotted curve, CTMC calculations (Schippers *et al* 1995). The experimental points (open circles) are taken from figure 3 of Schippers *et al*.

is stronger than capture to the 4p subshell. Overall, near this resonant energy, about 0.6% of the electrons are captured into $He^+(n = 2)$ state, 75% into $He^+(n = 3)$, and 25% into $He^+(n = 4)$. With the increase in the projectile energy, electron capture takes place into a band of electronic shells of the He^+ ion. It is clear from figure 4 that our Sturmian results for capture into the He^+ (4f) state are in good accord with the measured points. In particular, near the maximum, our results compare better than the other two theoretical results.

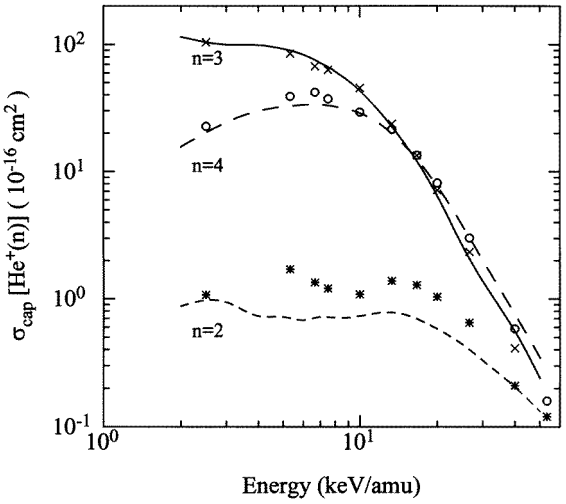

Figure 5. Partial electron transfer cross sections into the $n = 2$, 3 and 4 shells of the He^+ ion in the present energy range of 2–50 keV amu^{-1}. Present Sturmian results are shown by full ($n = 3$), long dash ($n = 4$) and short dash ($n = 2$) curves. The other theoretical results (Shingal *et al* 1987) are shown by crosses ($n = 3$), open circles ($n = 4$), and asterisks ($n = 2$).

The relative n shell dependence of the capture cross sections is shown in figure 5 along with the theoretical results of Shingal *et al* (1987). For the dominant channels ($n = 3$ and $n = 4$), the two calculations are in good agreement with each other, while agreement for the smaller $n = 2$ channel is not very good. Capture to the $n = 3$ shell dominates up to 15 keV amu^{-1}, while above this energy capture to the $n = 4$ shell is the strongest process. Electron transfer to the $n = 2$ shell is small at all energies considered here (although presumably it dominates at much higher energies, i.e. beyond the present energy regime), while the $n = 1$ channel is insignificant in the present energy region.

In order to see further the relative distribution of various magnetic subshells within an n manifold, in figures 6 and 7 we have illustrated 3ℓ (3s, 3p and 3d) and 4ℓ (4s, 4p, 4d and 4f) cross sections. It is interesting to note that the d subshell (3d and 4d) dominates over other subshells (ns, np, and 4f). The capture to the 4f subshell is quite important below about 7 keV amu^{-1}. We also note from figure 7 that the 4ℓ curves have structure below 15 keV amu^{-1}, while the 3ℓ curves (figure 6) are generally quite smooth.

3.2. Target excitation cross sections for $He^{2+} + Na$ (3s) collisions

The Na (3p) excitation is the dominant channel in He^{2+} collisions with sodium atoms in the present energy region. Figure 8 shows our cross sections for the excitation of the Na (3p) state in the energy range of 2–10 keV amu^{-1}, where the experimental data of Schlatmann *et al* (1992) are available for comparison. We have shown our results without cascading effects, as it is not clear whether the experimental data include such contributions. However, for this transition, the cascading effects are expected to be within 12–20% in this energy range. Also shown in figure 8 are the augmented AO results of Shingal *et al* (1987). First we notice from figure 8 that there is a remarkable similarity in the overall energy dependence of the Na (3p) excitation cross section between present Sturmian results and the experimental points. The dip structure observed in the measurements around 4 keV amu^{-1} is fairly well

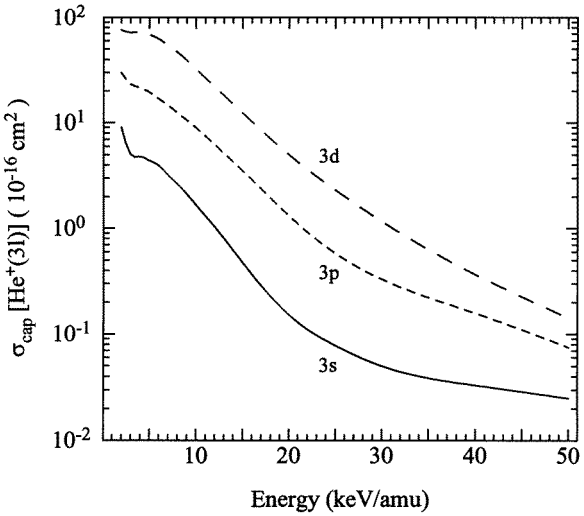

Figure 6. State-selective electron transfer cross sections into various subshells (3s, 3p, and 3d) of the $n = 3$ shell of He^+ in $He^{2+} + Na$ (3s) collisions using the present coupled-Sturmian-pseudostate method.

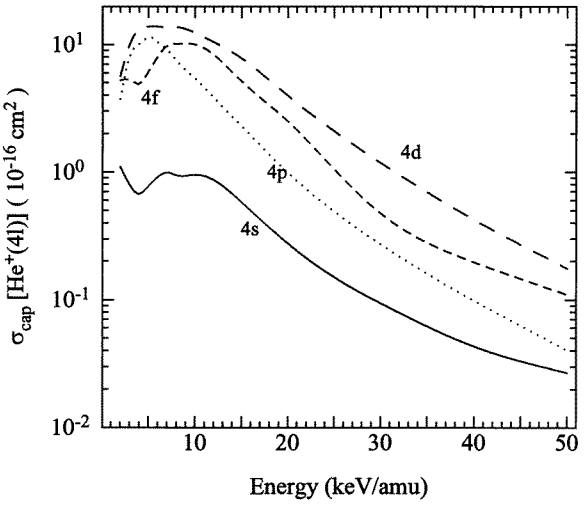

Figure 7. Cross sections as in figure 6, but for the capture into the 4s, 4p, 4d, and 4f subshells of the $n = 4$ shell of He^+.

reproduced in our calculations, while the augmented AO results of Shingal *et al* (1987) show little such behaviour.

At somewhat higher energies (15–70 keV amu^{-1}), Dehong *et al* (1989) have carried out optical measurements on the emission cross sections in the collisions of He^{2+} ions with Na atoms; their emission cross sections of the NaI $D_{1,2}$ line can be directly compared with the theoretical Na (3p) excitation cross sections. In figure 9, we have plotted our Na (3p) cross sections in the whole energy region (2–50 keV amu^{-1}) along with the experimental data of Schlatmann *et al* (1992) (2–9 keV amu^{-1}) and Dehong *et al* (1989) (15–50 keV amu^{-1}). Also shown in figure 9 are the calculated results of Shingal *et al* (1987). Quantitatively,

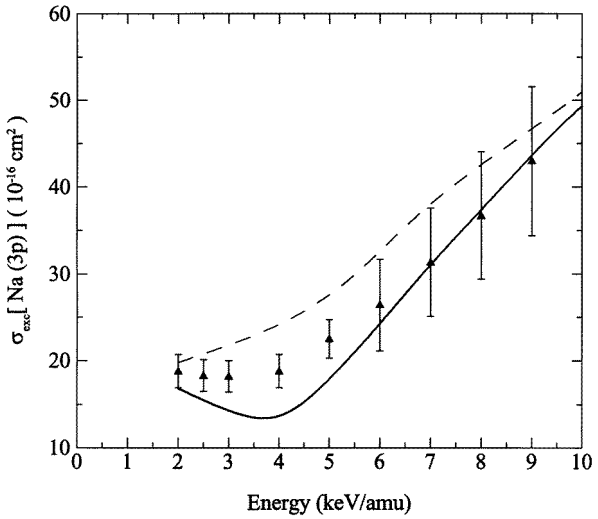

Figure 8. Na(3p) excitation cross sections (10^{-16} cm^2) for the He^{2+} + Na (3s) system at 2–10 keV amu^{-1}. Theory: present results, full curve; calculations of Shingal *et al* (1987), broken curve. The experimental points (triangles) are taken from Schlatmann *et al* (1992).

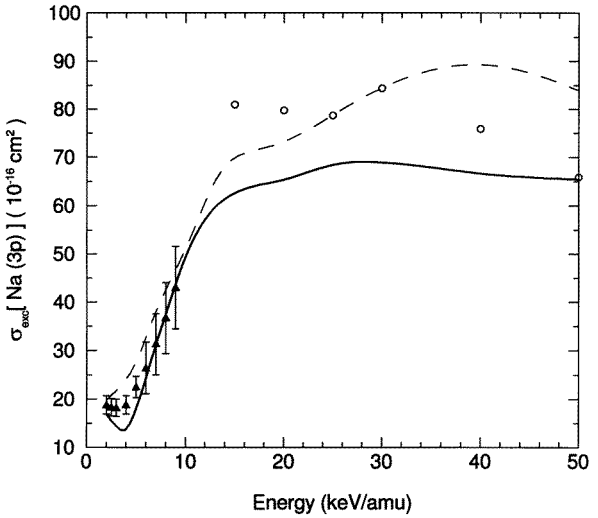

Figure 9. Cross section as in figure 8, but for the full energy range. The open circles are taken from the experimental data of Dehong *et al* (1989).

our Sturmian results seem to be in discrepancy with the experimental points of Dehong *et al*; however, there appears to be some agreement in the energy dependence of the cross section.

We now compare in figure 10 our Na (3d) excitation cross sections with the only other coupled-state results (Shingal *et al* 1987). There are no experimental data available for this transition. We see general agreement between the two sets of calculations employing different size and type of basis set in the coupled-state treatment of the problem. At the lower end of the energy range (below 10 keV amu^{-1}) our results are higher than the results

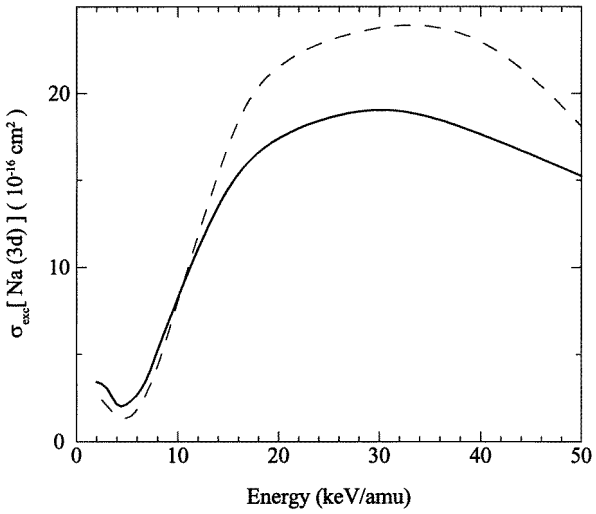

Figure 10. Na(3d) excitation cross sections (10^{-16} cm^2) for the He^{2+} + Na (3s) system at 2–50 keV amu^{-1}. Theory: present Sturmian results, full curve; results of Shingal *et al* (1987), broken curve.

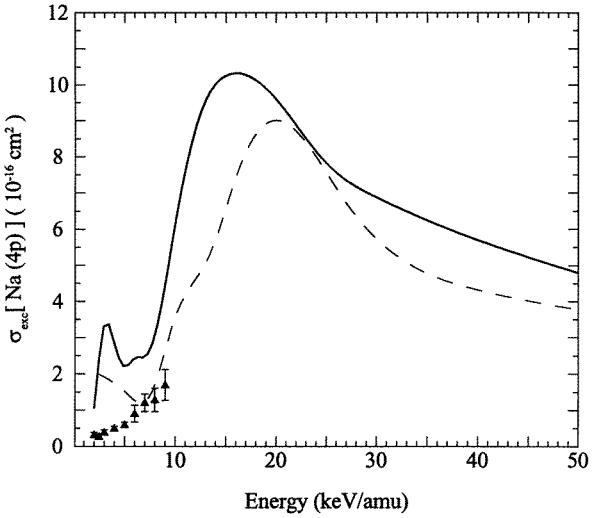

Figure 11. Cross sections as in figure 8, but for the Na (4p) state.

of Shingal *et al* (1987), while at higher energies, the present Sturmian values are lower (by about 20%) than these theoretical results.

Next we depict our Na (4p) and Na (4d) cross sections in figures 11 and 12, respectively. Also shown in these figures are the experimental data of Schlatmann *et al* (1992) and the calculations of Shingal *et al* (1987). Our results for the Na (4d) state are in excellent agreement with the experiment, while for the Na (4p) state, there is a large discrepancy between theory and experiment: our Sturmian curve shows peaking structure around 3 keV amu^{-1} which is not found in the measurements of Schlatmann *et al* (1992). The augmented AO calculation of Shingal *et al* (1987) is also in disagreement with the

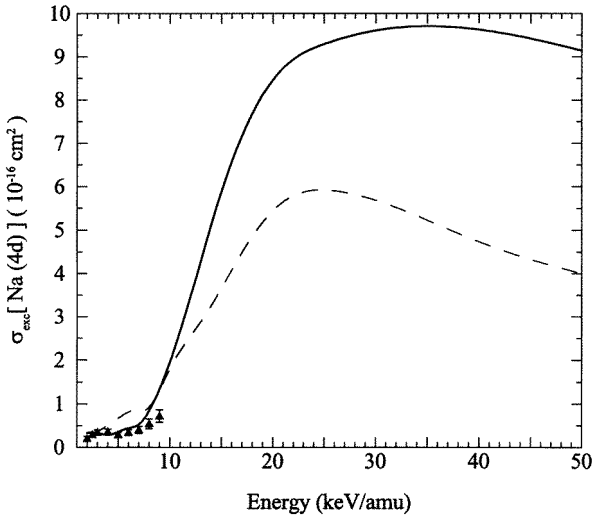

Figure 12. Cross sections as in figure 8, but for the Na (4d) state.

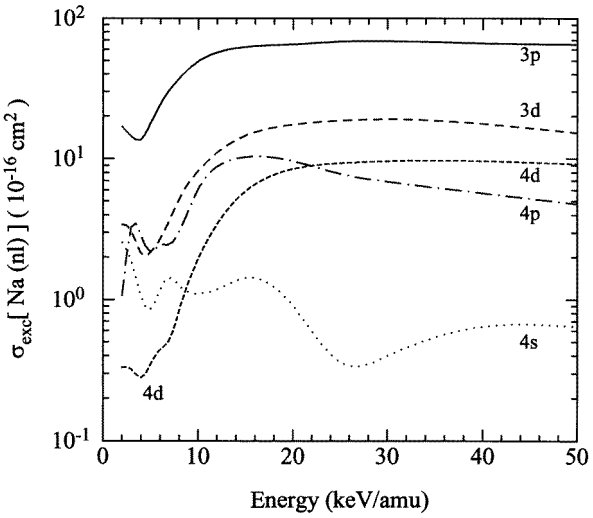

Figure 13. Target excitation Na($n\ell$) cross sections as a function of impact energy.

experiment for this excitation. In order to resolve the discrepancy for the Na (4p) cross section, another experimental study in this low energy region is needed. In the higher energy region (above 10 keV amu^{-1}), the Sturmian peak occurs around 16 keV amu^{-1}, while the AO calculations of Shingal *et al* (1987) predict this peak to be around 20 keV amu^{-1}.

In figure 13, we have shown the relative strengths of the Na (3p), Na (3d), Na (4s), Na (4p), and Na (4d) cross sections in the present energy range of 2–50 keV amu^{-1}. Excitation to the Na (3p) state dominates throughout, followed by Na (3d) excitation. Below 10 keV amu^{-1}, Na (4s) and Na (4p) are also significant; however, at higher energies, Na (4d) excitation becomes larger than the Na (4p) and Na (4s) excitations.

In figure 14, we have plotted cross sections for all three processes (electron transfer,

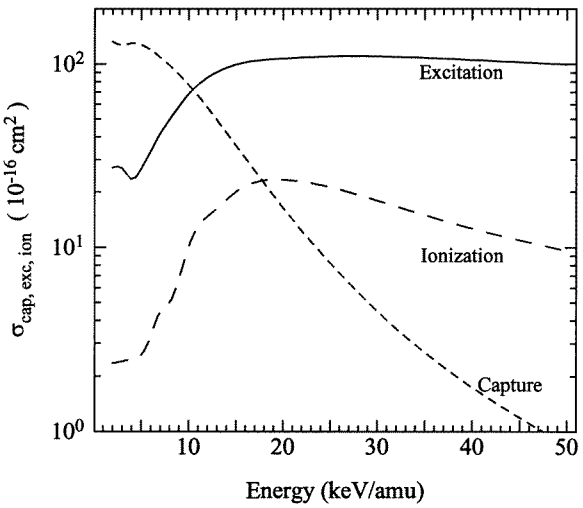

Figure 14. A comparison between total electron transfer, target excitation and total ionization cross sections for $He^{2+} + Na$ (3s) collisions calculated using the present Sturmian method in the energy region 2–50 keV amu^{-1}.

target excitation and ionization) as a function of impact energy (2–50 keV amu^{-1}). All three channels are seen to compete with each other in various regions of the present energy range. Below about 10 keV amu^{-1}, charge transfer (mainly into the $n = 3$ shell) is the main inelastic process, followed by Na excitation. At somewhat higher energies (above 15 keV amu^{-1}), target excitation (mainly into the 3p state) becomes the dominant channel, while the capture cross sections becomes very small, much smaller than even the ionization cross section. The ionization cross sections of DuBois (1986) for the $He^+ + Na$ (3s) system, not shown in figure 14, represent the sum of direct ionization to all the target states and involve large uncertainties (up to 50%) due to indirect procedures to obtain these values. Further, extracting numerical values from his small graphs would have added extra errors in the comparison. However the experimental ionization cross section values of DuBois appear to lie above the present values by a factor of about two and they have the same qualitative energy dependence. It would be interesting if some additional experimental data were available on the ionization process.

Finally, in table 3 we provide numerical values of target excitation cross sections in the 2–50 keV region obtained from our 74-state Sturmian calculation.

4. Conclusions

A coupled-Sturmian-pseudostate approach has been employed to calculate single electron transfer, target excitation and total ionization cross sections for $He^{2+} + Na$ (3s) collisions in the 2–50 keV amu^{-1} energy region. Present cross sections for total electron transfer, state-selective electron transfer [$He^+(n\ell)$], and target excitation from Na (3s) to Na (3p), Na (3d), Na (4p) and Na(4d) have been shown graphically along with other theoretical and experimental data in the 2–10 keV amu^{-1} range. (We have also provided all cross sections in tabular form.) We find that the present Sturmian AO method is generally quite successful in describing $He^{2+} + Na$ (3s) collisions in the present energy region. In particular, our results for total electron transfer, H($n = 3$) production, and excitation to Na (3p) and

Table 3. Present 74-state target excitation cross sections (10^{-16} cm^2) for the reaction $He^{2+} + Na\ (3s) \rightarrow He^{2+} + Na\ (n\ell)$.

keV amu^{-1}	Na (3p)	Na (3d)	Na (4s)	Na (4p)	Na (4d)	Total
2.0	16.80	3.43	2.53	1.07	0.33	27.16
3.0	14.28	3.05	1.83	3.34	0.32	26.85
4.0	13.66	2.11	1.04	2.81	0.28	23.43
5.0	17.88	2.16	0.85	2.19	0.35	26.74
6.0	24.20	2.70	1.18	2.43	0.44	33.42
7.0	31.00	3.70	1.43	2.46	0.52	41.79
8.0	37.35	5.20	1.25	3.05	0.84	49.90
10.0	49.30	8.23	1.10	6.11	1.95	68.58
12.5	58.52	11.70	1.22	9.21	3.88	87.69
15.0	62.55	14.53	1.42	10.25	5.89	99.30
20.0	65.30	17.40	0.90	9.59	8.47	107.01
25.0	68.38	18.58	0.36	7.82	9.29	109.98
30.0	68.89	19.04	0.40	6.87	9.60	110.01
40.0	66.60	17.63	0.64	5.70	9.62	105.22
50.0	65.40	15.24	0.64	4.79	9.14	99.56

Na (4d) states are in good agreement with the measured data. A large discrepancy, however, is observed between theory and experiment for the Na (4p) excitation cross section at low energies. Altogether, the present calculations reproduce most of the salient features observed in various processes for $He^{2+} + Na\ (3s)$ collisions.

Acknowledgments

This work was supported by the US Department of Energy, Office of Energy Research, Office of Basic Energy Sciences, Division of Chemical Sciences. The calculations were performed on Pennsylvania State University's IBM ES9000-740 computer.

References

Aumayr F, Gieler M, Unterreiter E and Winter H P 1991 *Eur. Phys. Lett.* **16** 557
Dehong Y, Jiarui L, Ziming L, Feng Y, Guangyan P, Duanwei W and Shiang S 1989 *Phys. Rev.* A **39** 2931
DuBois R D 1986 *Phys. Rev.* A **34** 2738
DuBois R D and Toburen L H 1985 *Phys. Rev.* A **31** 3603
Gieler M, Aumayr F, Schweinzer J, Koppensteiner W, Husinsky W, Winter H P, Lozhkin K and Hansen J P 1993 *J. Phys. B: At. Mol. Opt. Phys.* **26** 2137
Jain A and Winter T G 1995 *Phys. Rev.* A **51** 2963
Kumar A, Lane N F and Kimura M 1990 *Phys. Rev.* A **42** 3861
Schippers S, Boduch P, van Buchen J, Bliek F W, Hoekstra R, Morgenstern R and Olson R E 1995 *J. Phys. B: At. Mol. Opt. Phys.* **28** 3271
Schweinzer J and Winter H P 1990 *J. Phys. B: At. Mol. Opt. Phys.* **23** 3881
Schlatmann A R, Hoekstra R, Folkerts H O and Morgenstern R 1992 *J. Phys. B: At. Mol. Opt. Phys.* **25** 3155
Shingal R, Noble C J and Bransden B H 1987 *J. Phys. B: At. Mol. Phys.* **20** 793
Winter T G 1982 *Phys. Rev.* A **25** 697
——1987 *Phys. Rev.* A **35** 3799
——1993a *Phys. Rev.* A **47** 264
——1993b *Phys. Rev.* A **48** 3706